IL NUOVO CIMENTO Vol. 36 C, N. 4 Luglio-Agosto 2013
DOI 10.1393/ncc/i2013-11552-0

Communications: SIF Congress 2012

Sensitivity and spatial selectivity of transverse field RF surface coils: A theoretical and experimental study at 2.35 T

M. Alfonsetti(*)

Dipartimento di Medicina Clinica, Sanità Pubblica e Scienze della Salute, Università degli Studi di L'Aquila - via Vetoio, Coppito, 67100, L'Aquila, Italy and INFN, Gruppo Collegato L'Aquila, Sezione Laboratori Nazionali del Gran Sasso Assergi, 67100, L'Aquila, Italy

ricevuto il 15 Gennaio 2013

Summary. — A number of clinical magnetic resonance imaging/spectroscopy applications require a careful selection of the radiofrequency (RF) coil design to optimize the coil sensitivity and spatial selectivity in a well-defined region of interest. Small surface receiver RF coils are often used because they are highly sensitive, easy to construct, and provide spatial signal localization. We have analysed axial (square loop, SL) and transverse (figure-of-eight, FO8; butterfly, BC) RF field surface coils to study sensitivity and spatial selectivity along the coil axis. We have performed simulations with a finite element method at 100 MHz, and built prototypes of the coils. GE images were acquired in the presence of an oil phantom using a 2.35 T Bruker animal scanner. The results show a higher sensitivity and a more pronounced spatial selectivity along the coil axis with the transverse coils, as compared to the standard SL in the proximity of the RF coil plane. Moreover, a transmit flip angle calibration has been performed and a pronounced gain is obtained with the transverse coils. These features should be useful to optimize the RF coil sensitivity and spatial selectivity in a specific region of interest along the coil axis.

PACS 82.56-b – Nuclear magnetic resonance.
PACS 83.85-Fg – NMR/magnetic resonance imaging.
PACS 84.32-Hh – Inductors and coils; wiring.

1. – Introduction

In a number of clinical Magnetic Resonance Imaging (MRI) and Spectroscopy (MRS) applications a careful selection of the RF coil design is required to optimize the coil sensitivity and spatial selectivity in a well-defined region of interest (ROI). For example, MRS

(*) E-mail: maria.alfonsetti@univaq.it

clinical studies of human muscle diseases may require the acquisition of the NMR signal from a specific muscle and the attenuation of signal contamination from surrounding tissues. It has been shown that clinical MRS studies of the human calf muscles [1,2] require the enhancement of the signal from the gastrocnemius muscle and the attenuation of signal contamination due to fat and other muscles. Also, MRI human brain studies devoted to the identification of epileptogenic regions require increased signal-to-noise ratio (SNR) and high spatial resolution in a specific area of the brain [3].

Over the past 30 years or so, a great number of MRI and MRS studies have employed a variety of RF surface coils including axial [4-11] and transverse [12-20] RF field design. The standard square loop (SL) or circular loop RF coils present a B_1 field directed along the coil z-axis, with a maximum amplitude at the coil plane and a slow decrease toward zero along the coil axis. On the contrary, transverse-field RF coils produce a B_1 field that in the central region of the coil is parallel to the coil plane, and show a pronounced B_1 spatial selectivity in x-y planes parallel to the coil surface.

Transverse-field surface RF coils are made of a number of linear conductive elements, positioned in the central ROI, and connected by circular (or rectangular) return conductive paths. The so-called "butterfly coil" (BC) [21] presents two or more central crossing elements and shows the B_1 field maximum at the central position corresponding to the crossing of the elements. A detailed study of the dependence of the intrinsic SNR along the coil axis has been recently reported [22]. The so-called "figure-of-eight" (FO8) coil presents central linear currents directed along parallel directions and positioned at a given distance from each other. The FO8 coil presents a B_1 field distribution with a maximum along a central region corresponding to the linear elements. It was originally proposed for use in vertical-field MRI systems [12].

These specific features of transverse field RF coils are of considerable interest for spatially selecting and enhancing the MRI/MRS signal from a well-defined ROI of the sample. For example, we have shown that, using a two-element FO8 coil prototype tuned at 64 MHz, it is possible to avoid signal losses when the coil is oriented along specific directions within the MRI scanner [17]. Moreover, it was recently shown that the RF field spatial distribution of FO8 coils is advantageous for those *in vivo* MRS applications requiring spatial selectivity and signal enhancement from a specific anatomical region of the sample located at some depth from the surface [23,24].

From the above examples, it is evident that the specific spatial distribution of the RF field provided by transverse-field coils are of considerable interest for spatially selecting and enhancing the NMR signal from a well-defined ROI of the sample.

The aim of the present study was to analyse and compare axial (square loop, SL) and transverse (figure-of-eight, FO8; butterfly, BC) surface RF field coils to study the sensitivity and spatial selectivity along the coil axis. Simulations of the B_1 RF field have been performed with a Finite-Element Method (FEM) in the presence of a homogeneous model equivalent to the muscle tissue at 100 MHz. For experimental verification, prototypes of the SL, FO8 and BC coils matching the FEM models have been built, and MRI images were acquired in the presence of an oil phantom using a 2.35 T scanner.

2. – Materials and methods

To compare the B_1 spatial distributions of the transverse field and standard loop RF coils we have performed FEM simulations by using a commercial software (HFSS, Ansoft). The program allows to take account of the physical coils model (conductor geometry, connecting path, sources, frequency and materials). We have modelled (see

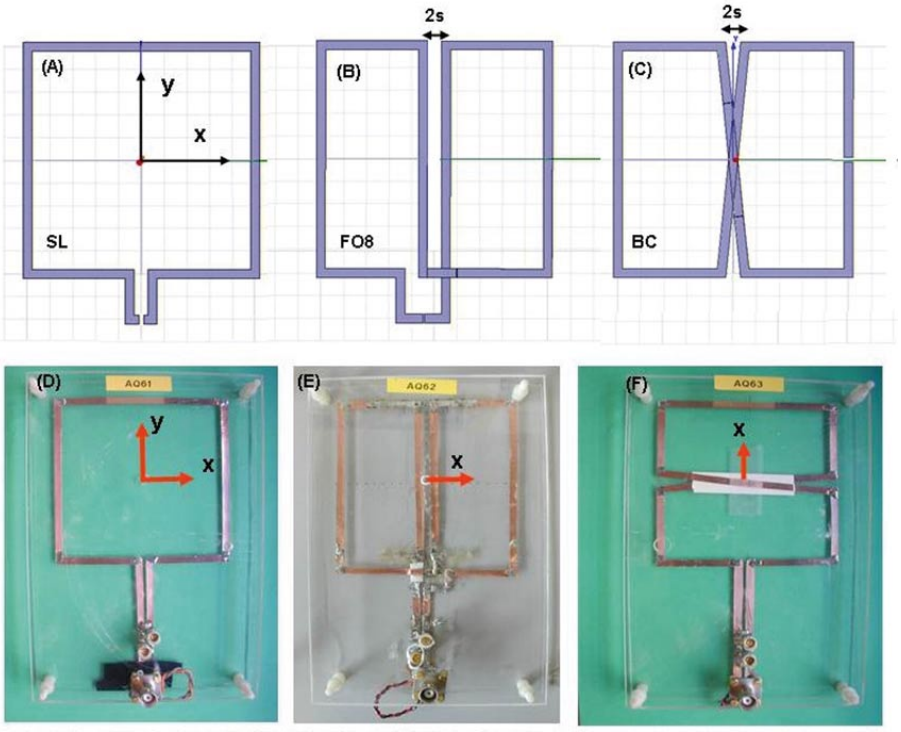

Fig. 1. – FEM model of SL (A), FO8 (B) and BC (C) coils. The corresponding prototypes are shown in (D), (E) and (F). Please note that the BC prototype (F) is rotated of 90° with respect to the FEM model for easy of presentation.

fig. 1A, B and C) square loop (SL), square butterfly (BC) and square figure-of-eight (FO8) coils having a size of 10 cm and tuned at 100 MHz, corresponding to a 2.35 T field. The RF coils were modelled with copper strips 4 mm width and 100 μm thickness. All the RF coils were simulated in the presence of a homogeneous model ($75\times75\times120\,\mathrm{mm}^3$) matching the muscle electrical characteristics at 100 MHz. For all simulation was used a tetrahedral mesh with second-order solution basis and adaptive mesh dimension with maximum size 15 mm, an adaptive solution with 12 cycles (scattering error ΔS per cycle less than 10^{-9}) and a radiation boundary condition fixed on a domain volume of $150 \times 150 \times 150\,\mathrm{mm}^3$.

Based on the simulation results, we have built and tested prototypes of the SL, BC and FO8 RF coils (fig. 1D, E and F) matching the FEM models. The coils were built and tested for ^{1}H MRI/MRS studies at 2.35 T. The RF coils were constructed on a Plexiglas substrate (thickness 2 mm) using adhesive copper strips (RS Components, Italy) of 4 mm width and 100 μm thickness.

Tuning and matching of the RF coils was achieved with non-magnetic high power chip capacitors (American Technology Ceramics, USA) and non-magnetic trimmer capacitor (Voltronics, USA; 1–16 pF). Tuning of the RF coils was achieved with a capacitor, C_t, connected in parallel with the inductive current path. A balanced circuit [25] was used for matching the SL and FO8 RF coils composed of two series chip capacitors, C_1, and a parallel trimmer capacitor, C_m. For the SL coil the tuning match was obtained with a trimmer capacitor C_m = 1–16 pF; for the adaptive match two series capacitors

$C_1 = 8.0\,\text{pF}$ and a parallel trimmer capacitor $C_\text{m} = 1$–$16\,\text{pF}$ were used. For the FO8 coil the tuning match was obtained with the a trimmer capacitors $C_\text{m} = 1$–$16\,\text{pF}$; for the adaptive match two series capacitors $C_1 = 2.78\,\text{pF}$ and a parallel trimmer capacitor $C_\text{m} = 1$–$16\,\text{pF}$ were used. The tuning match for the BC coil was obtained with a trimmer capacitor $C_\text{m} = 1$–$16\,\text{pF}$ connected in series to the conductive path; the adaptive match was obtained with a capacitor $C_\text{m} = 186\,\text{pF}$ and a trimmer capacitor (1–16 pF) connected in parallel to the coil.

A network analyser (HP8753A) was used to measure the power reflection coefficient (S_{11}) and the quality factor (Q) of the RF coils when loaded with an oil phantom ($75\times75\times120\,\text{mm}^3$). We found that the S_{11} coefficient (at the resonance frequency of 100.03 MHz) was better than -20 dB for all the RF coil prototypes. When empty, the measured Q values of the RF coil prototypes were 140 (SL), 150 (FO8) and 150 (BC); when loaded with the oil phantom, the measured Q values of the coil were 109 (SL), 112 (FO8) and 102 (BC). The oil phantom was used because it gives intrinsic coil B_1 field distribution [26].

Axial GE images (128×128, TE/TR = 7/700 ms, slice thickness = 4 mm, FOV = $14\,\text{cm} \times 14\,\text{cm}$, NEX=2) animal scanner (Bruker Biospec) in the presence of the oil sample. The RF coils were used in TX/RX mode. The acquisitions were performed for a number of nominal flip-angle values. From the modulus MRI images we calculated the average noise level (I_n) in a background region ($2.5\,\text{cm}^2$), for all coils. The signal amplitude (I_s) was calculated as the average in a ROI ($0.36\,\text{cm}^2$) positioned at about 5 mm from the coils. The signal-to-noise ratio (SNR) was calculated as $1.25 \times I_s/I_n$ [27]. To quantify the spatial selectivity obtained with the phantom, a comparison between the MR signal and the B_1 field distribution as calculated with the FEM was performed. Since for low flip-angle the MR signal of GE images is proportional to the square of the B_1 field [28], the signal profiles obtained along the coil z-axis were compared with the simulated distributions. The MR profiles were obtained as the mean signal in a ROI of $4.0\,\text{mm} \times 4.0\,\text{mm}$.

3. – Results and discussion

The simulated normalized B_1 field axial distributions for the coils along the z-axis are shown in fig. 2. It can be seen that the BC RF coil presents the most pronounced spatial selectivity in close proximity of the coil, with a rapid decrease as the distance from the coil increases. The B_1 amplitude is reduced to about 10% within 20 mm from the BC RF coil plane. The FO8 RF coil exhibits a B_1 field equal to zero on the coil plane, with a maximum at about 5 mm and a decrease to 10% of maximum within 40 mm from the FO8 coil plane. The SL coil presents a B_1 distribution with a maximum at the coil plane and a very slow decrease along the z-axis. The field simulation were performed within 50 mm from the coil plane, and in this range the B_1 field of the SL coil decreases to the 70% about of maximum. However, previous studies performed by using simulations based on the Biot-Savart law, show that the B_1 amplitude is reduced to about 10% within 100 mm from the coil plane.

It is worth noting that the square or circular loop coil have been successfully used for a number of *in vivo* MRI/MRS studies over a number of years. The pronounced selectivity of the transverse-field RF coils suggests that the FO8 and BC coils could be useful for a number of different applications in muscle, brain and derma tissues, that require high sensitivity within a ROI positioned at different depth in the tissues. The versatility of the FO8 coil design, that can be arbitrarily positioned with respect to the B_0 field in clinical MRI applications, has already been shown [17]. We have also shown that this RF

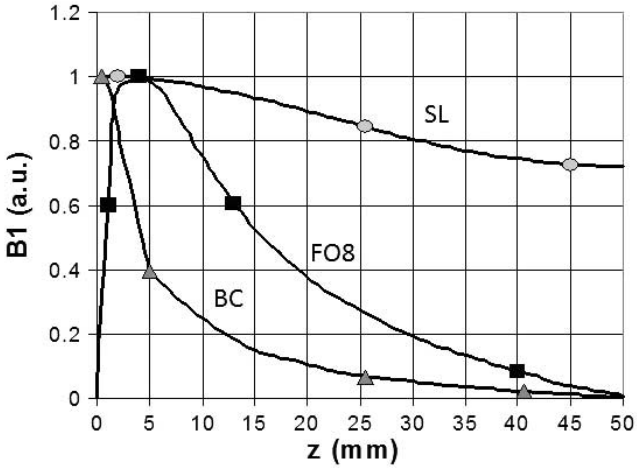

Fig. 2. – Simulated normalized B_1 field distribution along the coil z-axis for the SL (circle), FO8 (squares) and BC (triangles) coils. The data were obtained with the RF coils loaded with a model matching the human calf muscle tissue at 1.5 T.

FO8 coil can be helpful in improving the SNR of both water and lipids 1H NMR spectra acquired in the human calf in a relatively narrow region [23, 24]. Moreover, the more pronounced selectivity of the BC design, could be very useful for skin investigation [29] or non-destructive characterization of materials [30].

Figure 3 shows three typical axial GE images acquired in the presence of the oil phantom; the pronounced spatial selectivity along the coil z-axis is evident with the FO8 and BC coil, as compared to the standard SL. From the modulus images the measured noise values were about the same $(2.0 \cdot 10^3)$ for all coils. Figure 4 shows the SNR versus the nominal flip-angle for the three RF coils. We can see that the transverse-field coils require a smaller flip-angle to reach maximum SNR with respect to the SL, with a flip-angle gain of about a factor 2 for the FO8 coil and 3 for BC coil. In fact, the FO8 and the BC coils present the maximum SNR at a nominal flip-angle of 45° and 30° respectively, while the SL presents the maximum SNR at a nominal flip-angle of about 90°. Moreover,

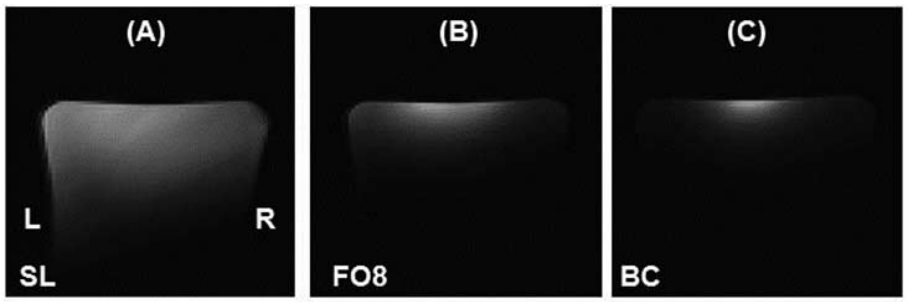

Fig. 3. – Axial GE images (128×128, TE/TR = 7/700 ms, thickness 4 mm, NEX = 2, FOV = 14 cm × 14 cm) obtained at 2.35 T with the SL (A), FO8 (B) and BC (C) RF coils loaded with the oil phantom ($75 \times 75 \times 120\,\mathrm{mm}^3$). The same FOV of $100 \times 100\,\mathrm{mm}^2$ is reported.

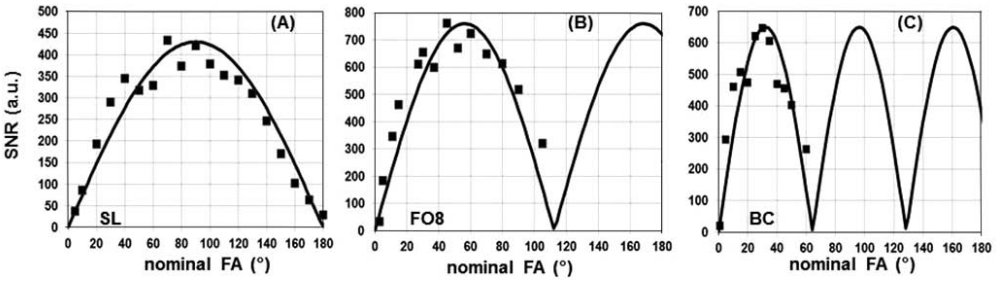

Fig. 4. – SNR *vs.* nominal flip-angle for the SL (A), FO8 (B) and BC (C) RF coils measured in a ROI ($0.36\,\mathrm{cm}^2$) selected on the central slice of the axial GE images of fig. 3, at about 5 mm from the coil planes.

from the absolute SNR values we found that the FO8 and BC coils give a useful SNR improvement of about a factor 1.75 and 1.50, respectively.

The comparison between the MR signal profiles along the coil z-axis and the simulated distributions are shown in fig. 5. As expected from theory, the SL coil shows a B_1 field with a maximum value on the coil plane and a slow decrease along the coil z-axis. We note, however, that the theoretical signal decrease is slower than the measured signal variation along the z-axis, with a maximum deviation of about 40% at 35 mm from the coil plane. On the contrary the FO8 coil shows a maximum B_1 field at a given distance from the coil plane, followed by a very fast decrease along the coil z-axis. The FO8 coil presents the maximum B_1 field value at about 6 mm, with an axial region of about 17 mm of B_1 field values within 50% of the maximum B_1 field value; the B_1 field value reaching the 10% amplitude at about 35 mm, in good accordance with theory. The BC coil shows a monotone and very fast decrease of the B_1 field value reaching the 10% amplitude at about 22 mm in accordance with theory, with an axial region of about 5 mm of B_1 field values within 50% of the maximum B_1 field value. A good agreement between the theoretical and measured RF field distribution of the transverse RF coils is observed, with a maximum deviation of about 10% within 35 mm from the coil plane.

In conclusion, the results presented here confirm that the RF field distribution of transverse field RF coils (FO8, BC) along the coil z-axis is spatially selective with respect

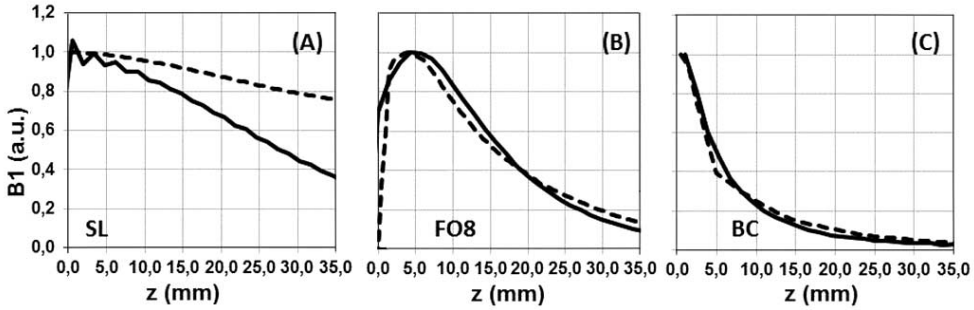

Fig. 5. – Comparison of the simulated B_1 field (dashed lines) and the GE MRI root square of the signal amplitude (continuous lines) along the z-axis for the SL (A), FO8 (B) and BC (C) RF coils, obtained with the oil phantom. The $z = 0$ corresponds to the RF coil plane.

to the standard SL. These features suggest that the transverse field RF coils could be useful for MRI applications requiring a good sensitivity/selectivity of specific region of interest located in close proximity of the surface. Specifically, given the characteristic spatial distribution of the transverse field RF surface coils, we anticipate benefits of the combined use with a standard volume RF coil [31-33] for perfusion imaging studies of the human brain. In fact, for example, a small size FO8 RF coil carefully positioned on the neck would allow efficient arterial blood spin labelling, while the use of the standard loop coil may suffer from a significant RF amplitude drop-off. The RF field spatial selectivity of the transverse field RF coils should also be of importance for parallel MRI techniques [34-36]. In fact, in these applications the efficiency of the signal encoding method depends on both the RF field distribution of the single coil element and the overall geometrical disposition of the array elements. Moreover, the features of the transverse RF coil design should also be of benefit in 31P MRS metabolic studies of the human calf muscles under force-controlled plantar flexion exercise [1, 2], where it is useful to increase the SNR in muscles close to the surface (*e.g.* gastrocnemius) and to attenuate spurious signal contribution from deeper muscles (*e.g.* soleus). Finally, transverse field RF coils should be useful in increasing the SNR and spatial resolution in skin MRI investigation [29] and non-destructive characterization of materials by single-sided NMR [30], where high sensitivity in planes close to the sample surface is mandatory.

* * *

I thank Prof. Marcello Alecci for his help with MRI data collection and useful discussions. I thank also Dr. Tomas Mazza for help with the FEM simulations.

REFERENCES

[1] Zaniol P., Serafini M., Ferraresi M., Golinelli R., Bassoli P., Canossi I., Aprilesi G. C. and Barbiroli B., *Phys. Med.*, **8** (1992) 87.
[2] Meyerspeer M., Krassak M., Kemp G. J., Roden M. and Moser E., *Magn. Reson. Mater. Phys.*, **18** (2005) 257, DOI: 10.1007/s10334-005-0014-y.
[3] Grant P. E., Barkovich A. J., Wald L. L., Dillon W. P., Laxer K. D. and Vigneron D. B., *Am. J Neuroradiol.*, **18** (1997) 291.
[4] Acherman J. J. H., Grove T. H., Wong G. G., Gadian D. G. and Radda G. K., *Nature*, **283** (1980) 167.
[5] Styles P., Scott C. A. and Radda G. K., *Magn. Reson. Med.*, **2** (1985) 402, DOI: 10.1002/mrm.1910020408.
[6] Brown T. R., Buchthal S. D., Murphy-Boesh J. and Nelson J. S., *J. Magn. Reson.*, **82** (1989) 629, 19111, USA DOI: 10.1016/0022-2364(89)90227-8.
[7] Taylor J. S., Vigneron D. B., Murphy-Boesh J., Nelson S. J., Kessler H. B., Coia L., Curran W. and Brown T. R., *Proc. Natl. Acad. Sci. U.S.A.*, **88** (1991) 6810, DOI: 10.1073/pnas.88.15.6810.
[8] Brooke N. S. R., Ouwerkerk R., Adams C. B. T., Radda G. K., Ledingham J. G. G. and Rajagopalan B., *Proc. Natl. Acad. Sci. U.S.A.*, **91** (1994) 1903.
[9] Doyle V. L., Payne G. S., Collins D. J., Verrill M. W. and Leach M. O., *Phys. Med. Biol.*, **42** (1997) 691, DOI: 10.1088/0031-9155/42/4/006.
[10] Woo D. C., Choe B. Y., Ha S. H. and Choi C. B., *Measurement*, **40** (2007) 615, DOI: 10.1016/j.measurement.2006.09.006.
[11] Meyerspeer M., Robinson S., Nabuurs C. I., Scheenen T., Schoisengeier A., Unger E., Kemp G. J. and Moser E., *Magn. Reson. Med.*, **68** (2012) , DOI: 10.1002/mrm.24205.
[12] Smith M. A. and Pye D. W., *Magn. Reson. Imag.*, **4** (1986) 455.

[13] Munsat T., Hooke W. M., Bozeman S. P. and Washburn S., *Appl. Phys. Lett*, **66** (1995) 2180, DOI: 10.1063/1.113939.
[14] Seton H. C., Hutchinson J. M. S. and Bussel D. M., *Magn. Reson. Mater. Phys.*, **8** (1999) 116.
[15] Wu Y. and Lieberman M. A., *Plasma Sources Sci. Technol.*, **9** (2000) 210, 10.1088/0963-0252/9/2/315.
[16] Alfonsetti M., Placidi G., Sotgiu A. and Alecci M., in *Proceedings of 20th Annual Scientific Meeting of the European Society for Magnetic Resonance in Medicine and Biology* (2003) S224.
[17] Alfonsetti M., Clementi V., Iotti S., Lodi R., Barbiroli B., Placidi G., Sotgiu A. and Alecci M., *Magn. Reson. Mater. Phys.*, **18** (2005) 69, DOI: 10.1007/s10334-004-0090-4.
[18] Alfonsetti M., Mazza T. and Alecci M., *Meas. Sci. Technol.*, **17** (2006) N53, DOI: 10.1088/0957-0233/17/10/n04.
[19] Alfonsetti M., PhD Thesis, Università di L'Aquila, L'Aquila, Italy (2004).
[20] Lim J. H., Kim K. N., Park J. K. and Yeom G. Y., *Phys. Plasmas*, **15** (2008) 083501, DOI: 10.1063/1.2967895.
[21] Mori I., US Patent 6,172,503 (2001).
[22] Kumar A. and Bottomley P. A., *Magn. Reson. Mater. Phys.*, **21** (2008) 41, DOI: 10.1007/s10334-007-0090-2.
[23] Alfonsetti M., Testa C., Iotti S., Malucelli E., Clementi V., Barbiroli B., Placidi G., Sotgiu A. and Alecci M., in *Proceedings of the 15th Meeting of the ISMRM, Toronto* (2008) 2600.
[24] Alfonsetti M., Testa C., Iotti S., Malucelli E., Clementi V., Barbiroli B., Placidi G., Sotgiu A. and Alecci M., *Open Spectros. J.*, **4** (2010) 1, DOI: 10.2174/1874383801004010010.DOI.
[25] Chen C. N., Hoult D. I., in *Biomagnetic Magnetic Resonance Technology* (IOP, Bristol) 1989.
[26] Alecci M., Collins C. M., Smith M. B. and Jezzard P., *Magn. Reson. Med.*, **46** (2001) 379, DOI: 10.1002/mrm.1201.
[27] Dietrich O., Raya J. G., Reeder S. B., Resiser M. F. and Schoenberg S. O., *J. Magn. Reson. Imag.*, **26** (2007) 375, DOI: 10.1002/jmri.20969.
[28] Haake E. M., Brown R. W., Thompson M. R. and Venkatesan R., *Magnetic Resonance Imaging: Physical Principles and Sequence Design* (Wiley, New York) 1999.
[29] Barral J. K., Bangerter N. K., Hu B. S. and Nishimura D. G., *Magn. Reson. Med.*, **63** (2010) 790, DOI: 10.1002.mrm.10353.
[30] Galante A., Savini A, Losito O., Alecci M., Dimiccoli V., De Maio P., Incampo A., Sebastiani P. and Sotgiu A., in *Proceedings of the IEEE International Workshop on Medical Measurements and Applications, Bari, Italy* (2011) 429.
[31] Silva A. C., Kim S.-G. and Garwood M., *Magn. Reson. Med.*, **44** (2000) 169, DOI: 10.1002/1522-2594(200008)44:2<169::AID-MRM1>3.0.CO;2-U.
[32] Barbier E. L., Silva A. C., Kim S.-G. and Koretsky A. P., *Magn. Reson. Med.*, **45** (2001) 1021, DOI: 10.1002/mrm1136.
[33] Fisher T., Breard M. E., Ludwing R. and Ferris C. F., in *Proceedings of the 12th Annual Meeting of ISMRM, Kyoto, Japan* (2004) 1573.
[34] Sodickson D. K. and Manning W. J., *Magn. Reson. Med.*, **38** (1997) 591, DOI: 10.1002/mrm1910380414.
[35] Pruessmann K. P., Weiger M., Scheidegger M. B. and Boesiger P., *Magn. Reson. Med.*, **42** (1999) 952, DOI: 10.1002/(sici)1522-2594(199911)42:5<952::AID-MRM16>3.0.CO:2-s.
[36] Katcher U., Börnert P., Leussler C. and Van Den Brink J. S., *Magn. Reson. Med.*, **49** (2003) 144, DOI: 10.1002.mrm.10353.